

# Quantum computing on long-lived donor states of Li in Si

V. N. Smelyanskiy<sup>1</sup>, A. G. Petukhov<sup>2</sup> and V. V. Osipov<sup>3</sup>

<sup>1</sup> *NASA Ames Research Center, Moffett Field, CA 94035*

<sup>2</sup> *Physics Department, South Dakota School of Mines and Technology, Rapid City, SD 57701*

<sup>3</sup> *Hewlett-Packard Company Laboratories 1501 Page Mill Road, 1L-12, Palo Alto, CA 94304*

We propose a quantum computer with charge-based qubits formed by the two lowest states of interstitial Li donor in Si under external stress. The excited state of a qubit can be extremely long-lived because its parity differs from that of the ground state. The strength of the phonon-induced resonant coupling between qubits has an unusual  $R^{-5}$  dependence on the interqubit distance  $R$  and qubits can be extremely well isolated from each other. A conventional  $R^{-3}$  law applies for transitions between the same-parity states providing a mechanism for 2-qubit operations with quality factor  $> 10^5$  at temperature  $\sim 10$  mK, and 100 nm interqubit distance (or 100 mK and 50 nm, respectively).

PACS numbers: 03.67.Lx, 89.70.+c

Keywords: Li, donors, silicon, quantum computing

A broad effort is currently underway to build a scalable quantum computer (QC) which consists of a large array of 2-level systems (qubits) and external controls for storage and coherent manipulation of quantum information. In practice, decoherence processes in qubits give rise to operational errors and require elaborate error-correction schemes. In the limit of large numbers of qubits fault-tolerant quantum computation requires [1] that the probability of an error in elementary quantum operations (gates) be no greater than  $10^{-5}$ - $10^{-6}$ . Errors this small are especially difficult to achieve when the QC is implemented as a solid-state device. However such implementation has a number of unique advantages related to scalability and the prospect of integration with state-of-the-art semiconductor device fabrication technology.

A number of solid-state quantum computer (QC) schemes have been proposed based on spin as quantum bits, including nuclear spin of  $^{31}\text{P}$  donors [2],  $^{29}\text{Si}$  nuclei [5] in Si matrix, electron spins in semiconductor heterostructures [6], and others. While spins are relatively

well isolated from the environment and characterized by long decoherence times, a natural limitation of the spin-based approach to quantum computing is the exponential falloff of the exchange interaction with inter-qubit distance. For nuclear donor spins a close (10-20 nm) separation between qubits is required [2]. This makes the fabrication process very challenging since it includes building control electrodes for individual addressing of each qubit and also detection of the state of each qubit using single-electrode transistors. The clock frequency for nuclear spin QC is relatively slow as well. The optically enhanced RKKY mechanism for electron spin-exchange [3] in semiconductor quantum dots allows for greater inter-qubit distances, but it is not clear at present how to make this QC scheme scalable [4].

An alternative approach in solid-state quantum computing is to perform the qubit encoding with charge degrees of freedom of electrons in quantum dots [7, 8], impurity centers [9, 10] and on a helium surface [11]. An especially interesting scheme [10] is based on acceptors in silicon that are characterized by a sub-KHz decoherence rate for qubits and uses a long-range virtual phonon-exchange mechanism for resonant inter-qubit coupling. However in most QC schemes based on charge-based qubits it is impossible to efficiently control the interaction strength between neighboring qubits while keeping interqubit separation small enough to maintain fast high-fidelity 2-qubit operations. Also decoherence-induced errors in charge-based qubits are still larger than in qubits based on nuclear spin.

In this paper we propose a new system for solid-state QC: shallow donors in Si that are free from the shortcomings mentioned above. The conduction band of Si has six valley minima  $\mathbf{k}_i$  located along six equivalent  $\langle 100 \rangle$  directions ( $i = \pm 1, \pm 2, \pm 3$ ) at about 85% of the distance  $2\pi/a_0$  to the Brillouin zone boundary [12] ( $a_0$  is a lattice constant for Si). The ground state of a shallow donor electron is 6-fold degenerate within the effective mass theory (EMT), however the valley-orbit interaction removes the degeneracy and gives rise to the splitting of the donor levels [13]. Exited states within the ground-state manifold are produced by splitting of 1s hydrogenic energy levels and decay predominantly via emission of acoustic phonons. The donor electron wave function can be written in the form  $\Psi_\mu(\mathbf{r}) = \sum_j \alpha_j^\mu \sum_{\mathbf{k}, \mathbf{G}} A_j(\mathbf{k} + \mathbf{G}) \psi_{\mathbf{k}}(\mathbf{r})$  where  $\mathbf{k}$  is a wave vector in the first Brillouin zone,  $\mathbf{G}$  is a reciprocal lattice vector,  $\psi_{\mathbf{k}}(\mathbf{r}) \equiv \langle \mathbf{r} | \mathbf{k} \rangle$  are Bloch functions and index  $\mu$  labels irreducible representations of the point group  $T_d$  that are characterized by the coefficients  $\alpha_j^\mu$ . Also  $A_j(\mathbf{k})$  are hydrogenic envelope functions in  $k$ -space that are strongly localized in the vicinity of the corresponding valley center  $\mathbf{k}_j$ .

The matrix elements of the electron-phonon interaction  $H_{\text{el-ph}}$  between the states of a donor electron are,  $\langle \Psi_\mu | H_{\text{el-ph}} | \Psi_{\mu'} \rangle = \sum_{\mathbf{q}\nu} V_{\mu\mu'}(\mathbf{q}\nu)(a_{\mathbf{q}\nu} + a_{-\mathbf{q}\nu}^\dagger)$ , where  $\nu$  is an index of phonon mode with wavevector  $\mathbf{q}$  and

$$V_{\mu\mu'}(\mathbf{q}\nu) = \sum_{|i|,|j|=1}^3 \alpha_i^\mu \alpha_j^{\mu'} \sum_{\mathbf{k},\mathbf{G}} A_i(\mathbf{k}) A_j(\mathbf{k} + \mathbf{q} + \mathbf{G}) M_{\mathbf{k}}(\mathbf{q}\nu). \quad (1)$$

here the summations are over  $i, j = \pm 1, \pm 2, \pm 3$  and  $M_{\mathbf{k}}(\mathbf{q}\nu)$  is the electron-phonon matrix element corresponding to the phonon mode  $\mathbf{q}\nu$  between Bloch functions  $|\mathbf{k}\rangle$  and  $|\mathbf{k} + \mathbf{q}\rangle$ . As usual, matrix elements  $V_{\mu\mu'}(\mathbf{q}\nu)$  determine the probability of transitions  $\mu \rightarrow \mu'$  per unit time:  $W_{\mu\mu'} = 2\pi/\hbar^2 \sum_{\mathbf{q}\nu} |V_{\mu\mu'}(\mathbf{q}\nu)|^2 \delta(\omega_{\mu\mu'} - \Omega_{\mathbf{q}\nu})$ , where  $\omega_{\mu\mu'}$  is a Bohr frequency for donor energy levels  $\mu$  and  $\mu'$  and  $\Omega_{\mathbf{q}\nu}$  is the frequency of the phonon mode  $\mathbf{q}\nu$ . Another important quantity determined by  $V_{\mu\mu'}(\mathbf{q}\nu)$  is the Rabi frequency of the resonant excitation transfer (RET) between a pair of donors with equal energies  $\hbar\omega_{\mu\mu'}$ :  $g_{\mu\mu'}(\mathbf{R}) = \frac{1}{\hbar^2} \mathcal{P} \sum_{\mathbf{q}\nu} |V_{\mu\mu'}(\mathbf{q}\nu)|^2 \exp(i\mathbf{q}\mathbf{R}) / (\omega_{\mu\mu'} - \Omega_{\mathbf{q}\nu})$ . Here  $\mathcal{P}$  stands for the principal value of the integral and donors are separated by a radius-vector  $\mathbf{R}$ . The probability  $W_{\mu\mu'}$  determines the qubit decoherence rate via phonon emission and, therefore, it is responsible for quantum gate and storage errors. The quantity  $g_{\mu\mu'}(\mathbf{R})$  is responsible for coherent inter-qubit coupling and ultimately for the clock frequency of a quantum computer.

For the long-wave acoustic phonons, that are the only relevant excitations in our frequency range,  $M_{\mathbf{k}}(\mathbf{q}\nu)$  reduces to [14]

$$M_{\mathbf{k}}(\mathbf{q}\nu) \simeq (\hbar/2\rho V \Omega_{\mathbf{q}\nu})^{1/2} \sum_{\alpha\beta} D_{\alpha\beta}(\mathbf{k}) q_\alpha e_\beta(\mathbf{q}\nu), \quad (2)$$

where  $\rho$  and  $V$  are the mass density and volume of the crystal respectively,  $D_{\alpha\beta}(\mathbf{k})$  is the deformation potential tensor,  $\mathbf{e}(\mathbf{q}\nu)$  is the phonon polarization vector, and  $\Omega_{\mathbf{q}\nu} = u_\nu q$  is a frequency of the acoustical mode  $\mathbf{q}\nu$ , with the speed of sound  $u_\nu$ . For  $q \ll |\mathbf{k}_i - \mathbf{k}_j|$  it seems reasonable to keep only intravalley terms with  $i = j$  in Eq. (1), and neglect small intervalley ( $i \neq j$ ) and umklapp ( $\mathbf{G} \neq 0$ ) terms corresponding to the overlap of the envelope functions from different valleys. The integral over  $\mathbf{k}$  in (1) corresponding to the  $i$ th valley is dominated by the small vicinity of the valley center  $\mathbf{k}_i$  where one can approximate

$$D_{\alpha\beta}(\mathbf{k}) \approx D_{\alpha\beta}(\hat{k}_i) = \Xi_u \hat{k}_{i\alpha} \hat{k}_{i\beta} + \Xi_d \delta_{\alpha\beta}, \quad (3)$$

where  $\Xi_u, \Xi_d$  are deformation potential constants and  $\hat{k}_i = \mathbf{k}_i/k_i$ .

We now discuss selection rules for intravalley transitions associated with inversion operation. Since the deformation potential  $D_{\alpha\beta}(\hat{k}_i)$  does not change under the inversion the transformational properties of  $\Psi_\mu(\mathbf{r})$  are determined by the parity of the multiple  $\alpha_j^\mu A_j(\mathbf{k})$  under the operation  $\mathbf{k}_j \rightarrow -\mathbf{k}_j$ . For example, parity is even for the  $s$ -type singlet or doublet states belonging to irreducible representations  $A$  or  $E$ , respectively. Also parity is odd in the case of  $s$ -type triplet states belonging to  $T_2$ . Similar parity classification can be applied to correct multivalley wave function  $\Psi_\mu(\mathbf{r})$  composed of  $p$ -type envelopes, etc. It follows from the above arguments and from Eq. (1) that contribution to  $V_{\mu\mu'}(\mathbf{q}\nu)$  from intravalley transitions connecting opposite parity states vanishes exactly. Analogous symmetry arguments lead to suppression of the  $1s(A) \rightarrow 1s(T_2)$  Raman transition in silicon donors [15]. We emphasize the immediate consequence of this fact: if one neglects intervalley transitions in (1) then *acoustic phonon transitions between the opposite-parity donor electronic states are forbidden in all orders in  $V_{\mu\mu'}(\mathbf{q}\nu)$ .*

Of special interest in this regard are transitions between odd parity  $1s(T_2)$  states and even parity  $1s(A)$  or  $1s(E)$  states. Intravalley processes are not possible and these transitions are dominated by the intervalley umklapp processes connecting opposite valleys  $\mathbf{k}_i$  and  $-\mathbf{k}_i + \mathbf{G}_i$  with  $\mathbf{G}_i = (4\pi/a_0)\hat{k}_i$ . This is due to the fact that these valleys are separated by a shortest distance from each other,  $\kappa_0 = 0.6\pi/a_0$ . In this paper we focus on the limiting case where intervalley transitions correspond to  $q_\nu/\kappa_0 \ll 1$  and can be described within EMT. In this case matrix element (1) is determined by the small tail of the envelope function  $A_i(\mathbf{k})$  in the opposite valley.

The above situation can be realized for a Li donor in silicon. Li is an interstitial impurity with  $T_d$ -site symmetry, it has an anomalous fivefold degenerate  $1s(E+T_2)$  ground state while the fully symmetric  $A_1$  state lies above, with the splitting between the states conventionally denoted by  $6\Delta_c = 1.76$  meV [16]. This sequence of levels is inverted as compared to that observed for group-V donors. If a uniaxial compressive stress  $F_z$  is applied along the  $\langle 001 \rangle$  direction the site symmetry of the donor is reduced from  $T_d$  to  $D_{2d}$ , and the ground state level is split into three levels as shown in Fig.1 [12, 16, 17]. New ground state  $|0\rangle$  has odd parity with only nonzero valley-orbit symmetry coefficients  $\alpha_{\pm 3}^0 = \pm \frac{1}{\sqrt{2}}$ . The first excited state  $|1\rangle$  has even parity and  $\alpha_i^1 = (b, b, b, b, a, a)$ , coefficients  $a \equiv a(\epsilon)$  and  $b \equiv b(\epsilon)$  can be found in [17]. At small magnitude of the applied stress  $|F_z|$  they take a simple form:

$a = (6 + \varepsilon)/6\sqrt{3}$ ,  $b = (3 - \varepsilon)/6\sqrt{3}$  where

$$\varepsilon = \frac{1}{3\Delta_c} \Xi_u (s_{11} - s_{12}) F_z, \quad |\varepsilon| \ll 1, \quad (4)$$

and  $s_{11}$ ,  $s_{12}$  are elastic compliance constants. The third energy level in Fig. 1 corresponds to a triplet of states that consists of an even parity state  $|2\rangle$  corresponding to  $\alpha_i^2 = \frac{1}{2}(1, 1, -1, -1, 0, 0)$  and odd parity states  $|3\rangle$ ,  $|4\rangle$  whose only nonzero coefficients are  $\alpha_{\pm 1}^3 = \alpha_{\pm 2}^4 = \pm \frac{1}{\sqrt{2}}$ .

The unique arrangement of shallow donor eigenstates with the ground and first excited states having opposite parities provides a basis for the new quantum computing scheme where a pair of states  $|0\rangle$  and  $|1\rangle$  is used to encode a qubit with an extremely long decoherence time. The probability of one-phonon transition  $W_{10}$  can be computed using (1)-(3), the valley-orbit symmetry coefficients  $\alpha_i^\mu$ , and calculating  $A_j(\mathbf{k})$  as a Fourier transform of a corresponding Kohn-Luttinger envelope function [13]

$$W_{10} \equiv \tau_{10}^{-1} = \frac{2}{35} \cdot \frac{a^2(\epsilon)(a_{\parallel}\kappa_0)^2}{[1 + (a_{\parallel}\kappa_0/2)^2]^6} \cdot \frac{\Xi_u^2 \omega_{10}^5 a_{\parallel}^2}{\pi \hbar \rho u_t^7}, \quad (5)$$

here  $\kappa_0 = 0.6\pi/a_0$ . We note an unusual dependence of the probability of the “forbidden” transitions between the opposite parity states on the phonon frequency,  $W_{10} \propto \omega_{01}^5$ . This is in contrast with the conventional dependence for the “allowed” transitions between the same parity states [10] such as 1-2 transition,  $W_{21} \propto \omega_{21}^3$ .

In designing our scheme for quantum computation we will make use of the fact that by varying the local pressure  $F_z$  one can change the frequencies  $\omega_{\mu\mu'}$  and therefore lifetimes  $\tau_{\mu\mu'}$  of the corresponding transitions. As seen on the insert of Fig. 1 there is a dramatic difference between the allowed and forbidden transition probabilities which exceeds seven orders of magnitude at  $\varepsilon = 1$ . For  $\varepsilon \leq 0.5$  the lifetime of the state  $|1\rangle$  becomes extremely large exceeding 0.01 s and reaches minutes and even hours for  $\varepsilon < 0.1$  ( $\hbar\omega_{01} < 0.17$  meV). One could choose a level separation in a qubit by setting  $\varepsilon \simeq \varepsilon_0 = 0.34$  which corresponds to a moderate stress of  $\sim 2.7 \cdot 10^7$  dyn/cm<sup>2</sup> and  $\hbar\omega_{10} \simeq 0.1$  meV (24 GHz). This gives a storage time of a qubit  $\tau_{10} \simeq 67$  ms that exceeds by more than  $10^5$  times the characteristic time-scales for one- and two-qubit operations (see below). On the other hand the inter-level separation of 0.1 meV allows computations to be performed at relatively high temperature  $T^*$  exceeding 100 mK [18].

Similarly to (5) one can compute the RET Rabi frequency for a given pair of donors separated by a radius-vector  $\mathbf{R}$ . In the case of a resonance between the forbidden transitions 0-1 one has

$$\frac{g_{10}(\mathbf{R})}{W_{10}} = \frac{315}{16} \left( 3 - \frac{u_t^2}{u_l^2} \cdot (4\sigma + 5) \right) \cdot \left( \frac{u_t}{\omega_{10}R} \right)^5 \quad (6)$$

( $\sigma = \Xi_u/\Xi_d$ ). We emphasize a very steep falloff of the RET Rabi frequency with donor-donor separation,  $g_{10} \propto R^{-5}$ . For the allowed transitions between the states with the same parity RET occurs over much larger distances [10], e.g.,  $g_{21}(\mathbf{R}) \sim 1/R^3$  (see Fig. 1 and also discussion below). *The very steep decrease of  $g_{10}(\mathbf{R})$  with  $R$  effectively allows the isolation of different qubits from each other in a controllable way.* For example, even at perfect resonance for a pair of 1-0 transitions separated by  $R=50$  nm, the coupling is very small,  $g_{10} \simeq 145$  Hz. By adjusting the magnitudes of a locally applied stress in neighboring qubits one can detune their 1-0 transition frequencies from resonance and reduce the coupling even further.

To implement two-qubit gates for a given pair of neighboring donors we use RET between their transitions  $2 \rightarrow 1$ . Then the quality factor for a 2-qubit gate is determined by the ratio

$$\frac{g_{21}(\mathbf{R})}{W_{21}} = \frac{5}{16} \left[ 2 + 7 \left( 1 - \frac{u_t^2}{u_l^2} \right) \right] \left( \frac{u_t}{\omega_{21}R} \right)^3, \quad (7)$$

(we have assumed  $\mathbf{R} \parallel \langle 100 \rangle$ ). Unfortunately, at  $\varepsilon = \varepsilon_0$  and  $R = 50$  nm, the ratio  $g_{21}/W_{21} < 1$ . It means that the qubit in state  $|2\rangle$  will decay before transferring its energy to another qubit in state  $|1\rangle$ . To achieve high-fidelity 2-qubit gates, much smaller interlevel distances are required. Therefore whenever we need to execute a 2-qubit gate we will adiabatically reduce the stress  $\varepsilon(t)$  from  $\varepsilon_0 = 0.34$  to  $\varepsilon_2 \simeq 0.002$  ( $F_z \sim 1.3 \cdot 10^5$  dyn/cm<sup>2</sup>) which will set the transition frequency to  $\omega_{21}/2\pi \simeq 0.24$  GHz. In this case the characteristic time for a 2-qubit gate,  $2\pi/g_{12} \simeq 0.2$   $\mu$ sec, is much shorter than the relaxation time  $\tau_{21} \simeq 3$  msec and therefore the donor electron levels will not be thermally repopulated during RET despite  $k_B T^* / \hbar \omega_{12} \simeq 8$ . As soon as the two-qubit gate is executed the qubits will be adiabatically returned into their high-stress state. With this choice of parameters the QC clock frequency is  $g_{21}/2\pi \simeq 5.2$  MHz and the quality factor of a 2-qubit gate  $g_{21}/W_{21} \sim 10^5$ . By lowering the operational temperature  $T^* < 100$  mK we can significantly increase the quality factor or/and increase the interqubit separation  $R$  as shown in Fig. 1. To implement 1-qubit gates we apply a small-amplitude periodic external stress  $\mathbf{F}^{ac}(t)$  of frequency  $\omega$  simultaneously in the  $\langle 001 \rangle$  and  $\langle 110 \rangle$  directions normal to the linear chain of qubits (see Fig. 2). This stress

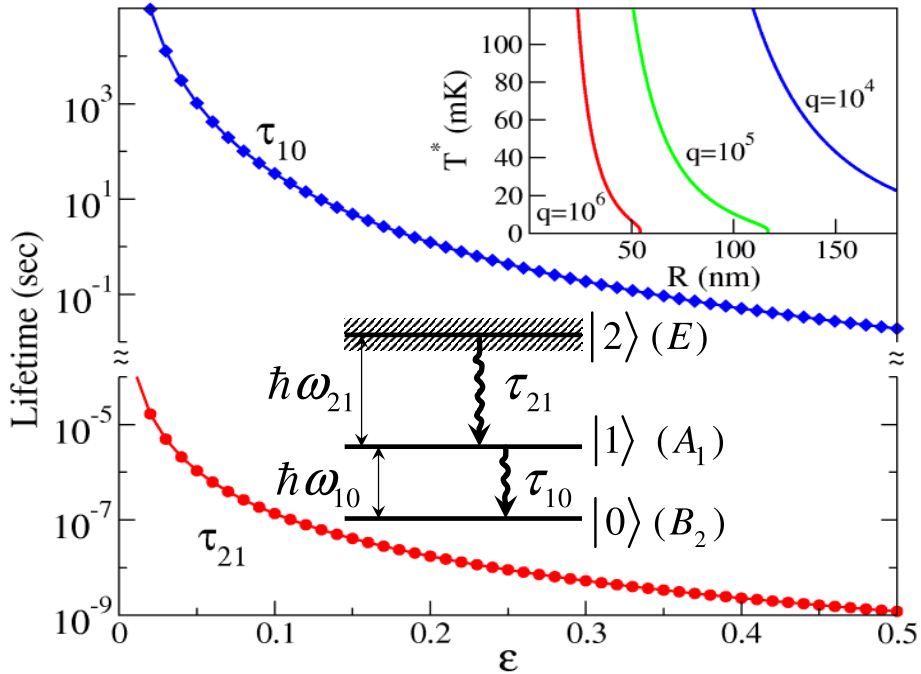


FIG. 1: Dependence of the lifetimes  $\tau_{10}$ ,  $\tau_{21}$  of the first two excited states of Li donor in Si on  $\varepsilon$ . The insert in the middle shows the energy levels of an isolated Li donor in Si under the compressive force  $\mathbf{F} \parallel \langle 001 \rangle$ . Bohr frequencies  $\omega_{10} = \omega_{21}/2 = \varepsilon \Delta_c / \hbar$ . The insert in the upper right corner displays the dependence of the operational temperature  $T^*$  on the inter-qubit distance  $R$  for different values of the quality factor  $q$  and  $F_z = 1.3 \cdot 10^5 \text{ dyn/cm}^2$  ( $\hbar \omega_{12} = 0.001 \text{ meV}$ )

will excite coherent longitudinal acoustic phonons in the two directions. It follows from the form of the coefficients  $\alpha_i^\mu$  that in this case undesirable modulation of inter-level separations can be removed by adjusting the amplitudes of the two orthogonal components of  $\mathbf{F}^{ac}(t)$ :  $F_{110}^{ac} = \sqrt{8}/3 F_{001}^{ac}$ . Then for the diagonal elements of the driving Hamiltonian  $H(t)$  one has  $H_{00}(t) - H_{11}(t) = H_{11}(t) - H_{22}(t)$ . The sole effect of  $\mathbf{F}^{ac}(t)$  will be to resonantly drive the transition 0-1 in a selected donor. In the case  $\omega \approx \omega_{01}$  the evolution of a qubit state will be controlled by an effective Hamiltonian

$$\tilde{H} = \hbar(\omega - \omega_{01}) \sum_{i=0,1} (-1)^i |i\rangle\langle i| + \tilde{H}_{01}(|0\rangle\langle 1| + h.c.), \quad (8)$$

where  $\tilde{H}_{01} = 128/\sqrt{6} F_{001}^{ac} S_{11} (\Xi_u + \Xi_d) \kappa_0 a_\parallel^2 \omega_{01} / u_l$ . By adjusting the parameters  $\omega - \omega_{01}$  and  $\tilde{H}_{01}$  various 1-qubit gates can be implemented. In a similar way one can resonantly excite the 1-2 transition required for 2-qubit operations. Another option consists of growing the

structure in the  $\langle 1\bar{1}0 \rangle$  rather than the  $\langle 001 \rangle$  direction. In this case a stress  $F_{111}^{ac}(t)$  applied in an orthogonal direction  $\langle 111 \rangle$  will drive the transitions in question without perturbing the inter-level spacing to the first order (simple dilation).

The optical absorption linewidth for the  $2p_{\pm}$  Li donor state in Si is  $\simeq 0.01$  meV due to the “lifetime effect” [17]. Readout is performed at a stress value  $\varepsilon = \varepsilon_0$  ( $\hbar\omega_{01}=0.1$  meV), using resonant optical excitation to the  $2p_{\pm}(+)$  level of the deformation-split  $2p_{\pm}$  manifold. A linearly polarized electric field  $\mathbf{E} \parallel \langle 001 \rangle$  will cause the transition to  $2p_{\pm}(+)$  from the state  $|1\rangle$  but **not** from the state  $|0\rangle$  [17]. By detecting an emitted photon during the subsequent decay transition, or dipole moment of  $2p_0(-)$  state ( $\sim 20 \text{\AA}e$ ) it will be possible to determine whether the state  $|1\rangle$  was occupied prior to excitation.

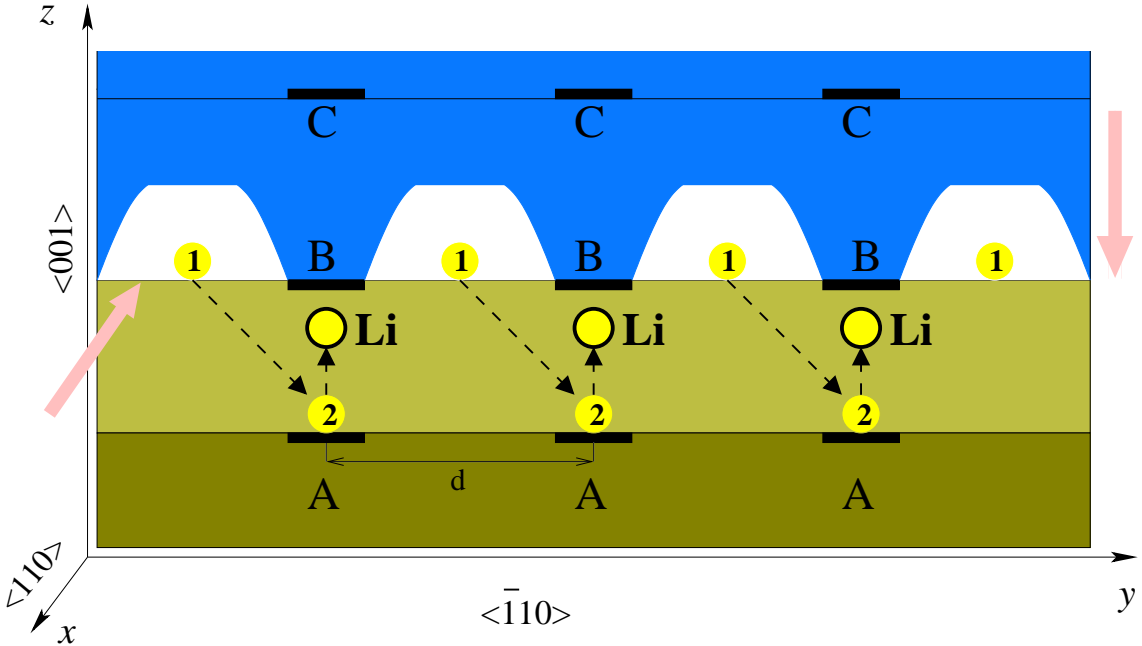


FIG. 2: Schematic view of the Si:Li-based quantum computer

The fabrication process of a Si:Li quantum computer shown in Fig. 2 proceeds in the following main steps. Electrodes  $A$  are placed on the surface of the Si substrate a distance  $d \sim 50\text{--}100$  nm from each other (inter-qubit distance in the QC). A thin epitaxial layer of high purity Si is grown on the Si substrate oriented with the  $(x, y)$  plane corresponding to the  $\langle 110 \rangle$  and  $\langle \bar{1}10 \rangle$  crystallographic directions. Electrodes  $B$ , as well as the readout electronics (including SET) connected to them are formed on the surface of the Si layer. A negative

potential is applied to the electrodes  $A$ . Atoms of Li are sequentially deposited between the electrodes  $B$ . They are attracted to the nearest  $A$ -electrodes (the process is shown with arrows from 1 to 2 in Fig. 2). This process is possible because Li atoms in Si are ionized and have very high mobility at room temperatures [17]. A piezoceramic film is etched to have a row of columns (of width  $\sim 30\text{-}40\text{nm}$ ) separated by arches along one edge. It is placed with the columns in contact with the electrodes  $B$ . This enables the generation of a local pressure in the  $\langle 001 \rangle$  direction. Each electrode  $C$  inside of the piezoceramic film is placed a distance  $\sim d$  from the neighboring  $B$ -electrode. The system temperature is decreased and simultaneously a negative voltage is applied to the electrodes  $B$  so that the Li ions begin to move toward their final operational positions (black circles with a yellow interior in Fig. 2). At the end, the system is cooled to the low operational temperature. In order to control the external pressure parallel to the  $\langle 110 \rangle$  axis an analogous piezoceramic structure should be attached to the side of the high-purity Si plate so that the columns fall on the  $yz$ -plane in Fig.2 (directions of mutually orthogonal external pressure forces are shown with pink arrows in Fig. 2).

In conclusion, our QC scheme qubits consisting of two opposite-parity 1s states of Si:Li donors do not involve spin and dipole moment degrees of freedom. They can be extremely long-lived and well isolated from each other and from electrode noise. Resonant acoustic-phonon exchange between qubits enables quantum operations with very high quality factor comparable with that of solid-state nuclear-spin QC, but allows for much greater temperatures and interqubit separation. We note in passing that the possibility for a huge qubit storage time  $\tau_{10} \gtrsim 1$  sec (at  $T^* \gtrsim 10$  mK) can be advantageous for quantum computation with parallel processors [19].

We acknowledge valuable discussions with M. Dykman, B. Golding (MSU, East Lansing) and C. Williams (JPL, Pasadena). This work was supported in part by: (V.S.) NASA Revolutionary Computing program; (A.P.) NSF grant DMR-0071823 and the Naval Research Laboratory through ASEE-ONR Summer Faculty Program.

---

[1] J. Preskill, in *Introduction to quantum computation and information*, ed. by H.K. Lo, S. Popescu, T. Spiller (World Scientific, Singapore, 1998), pp. 213-270.

- [2] B. E. Kane, Nature 393, 133 (1998);
- [3] C. Piermarocchi, et al., Phys. Rev. Lett. **89**, 167402 (2002).
- [4] X Li et al. 2003 Science 301 809.
- [5] T.D. Ladd, *et al.*, Phys. Rev. Lett. 89, 017901 (2002).
- [6] D. Loss and D.P. DiVincenzo, Phys. Rev. A 57, 120 (1998).
- [7] G. Chen, *et al.*, Science 289, 1906 (2000);
- [8] T.H. Stievater, *et al.*, Phys. Rev. Lett. 87, 133603 (2001).
- [9] M.D. Lukin and P.R. Hemmer, Phys. Rev. Lett. **84**, 2818 (2000).
- [10] B. Golding and M. I. Dykman, cond-mat/0309147.
- [11] P. Platzman, M.I. Dykman, Science **28**, 1967 (1999).
- [12] G.D. Watkins and F.S. Ham, Phys. Rev. B **1**, 4071 (1970).
- [13] W.Kohn and J.M.Luttinger, Phys. Rev. **98**, 915 (1955).
- [14] P. Vogl, Phys. Rev. B. **13**, 694 (1976).
- [15] K. Jain, S. Lai and M. V. Klein, Phys. Rev. B **13**, 5448 (1976).
- [16] R.L. Aggarwal, et al., Phys. Rev. **138**, A 882 (1965).
- [17] C. Jagannath and A.K. Ramdas, Phys. Rev. B **23**, 4426 (1981).
- [18] In addition to the lifetime  $\tau_{01}$  one also needs to consider dephasing time [10]  $\tau_{01}^{\text{dp}}$  due to quasi-elastic phonon scattering off donors. One can show that  $\tau_{01}^{\text{dp}} = \tau_0(T/T_0)^{11}$  where  $\hbar/\tau_0 \sim 1$  ev and  $T_0 = \hbar u_t/a_{\perp} = 19$  K, so that at  $T=100$ mK the dephasing time is extremely large.
- [19] R.M. Gingrich, C.P. Williams, and N. J. Cerf, Phys. Rev. A **61**, 052313 (2000).